Downlink Beamforming for WCDMA based on Uplink Channel Parameters

Christopher Brunner,[1, 2] *Michael Joham,*[2] *Wolfgang Utschick,*[2] *Martin Haardt,*[1] *and Josef A. Nossek* [2]

1. Siemens AG, ICN CA CTO 71
Hofmannstr. 51, D-81359 Munich, Germany
Phone / Fax: +49 (89) 722-29480 / -44958
E-Mail: Martin.Haardt@icn.siemens.de

2. Institute for Network Theory and Circuit Design
Munich Univ. of Technology, D-80290 Munich, Germany
Phone / Fax: +49 (89) 289-28511 / -28504
E-Mail: Christopher.Brunner@ei.tum.de

***Abstract* – The downlink spectral efficiency of third generation mobile radio systems is especially important since several services will be asymmetric, i.e., on the average the downlink data rates will be higher than on the uplink. We propose to utilize adaptive antennas at the base stations because spatial interference suppression is able to reduce the near-far effect caused by high data rate connections in the downlink of single-user detection DS-CDMA systems. The algorithm that calculates the downlink beamforming vectors takes into account the correlation properties of the spreading and scrambling codes. It is also based on estimates of the downlink channel parameters in terms of the dominant directions of arrival, corresponding delays, and corresponding medium-term average path losses. A non-linear minimization problem with non-linear constraints is set up, where the total transmit power is minimized while each mobile is provided with the required signal to interference and noise ratio (SINR) at the output of its rake receiver.**

1 Introduction

Future mobile communication systems require a significant increase in capacity to accommodate the growing number of users and to allow new services with higher data rates and a variety of quality of service requirements. The proposed concepts for third generation mobile radio systems allow an easy and flexible implementation of new and more sophisticated services. Recently, ETSI SMG selected the TD-CDMA concept for time-division duplex (TDD) systems and the WCDMA concept for frequency-division duplex (FDD) systems[1] [5]. Adaptive antennas exploit the inherent spatial diversity of the mobile radio channel and perform spatial interference suppression. Therefore, they are an important technology to meet the high spectral efficiency and quality requirements. We have investigated the uplink data detection in WCDMA utilizing adaptive antennas at the base station (BS) in [2, 3].

In this paper, we focus on the downlink of WCDMA. In general, high data rate connections on the downlink of WCDMA must be transmitted with more power than low data rate connections in order to compensate for the lower processing gain. If the spreading factors differ significantly, the near-far effect may degrade the performance of the low data rate mobiles significantly. Downlink beamforming, cf. Figure 1, leads to spatial interference suppression and, therefore, reduces the near-far effect. Moreover, fast fading can be mitigated by exploiting the spatial transmit diversity. In the sequel, we assume that the BS is enhanced with an antenna array. The mobiles are equipped with a single antenna and a conventional maximum ratio combining rake receiver [11]. Notice that the simplicity of the mobile is very important from an economic point of view.

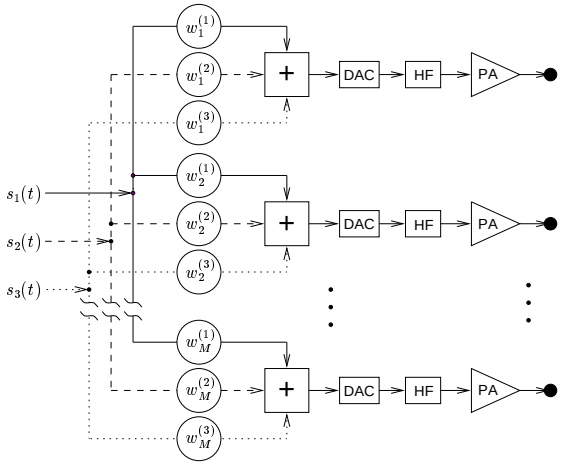

Figure 1: Illustration of downlink beamforming for K=3 users and M antenna elements.

Depending on the service, each mobile requires a certain transmission rate and bit error ratio. These parameters set the target SINR required at the output of the mobile maximum ratio combining rake receiver. In [7], a downlink beamforming approach is introduced which provides each user with a given SINR. To this end, a complex nonlinear constrained optimization problem is set up and several approximations are discussed. However, the users in [7] are separated by space only, whereas for WCDMA, separation takes place in the space *and* the code domain. Therefore, the calculation of the downlink beamforming vectors for WCDMA should also consider the auto- and cross-correlation properties of the spreading and scrambling codes in addition to the (medium-term) downlink

[1]This solution has been contributed to the International Telecommunication Union - as the European proposal for IMT-2000 transmission technology.

channel parameters. The intercell interference and thermal noise are considered as well. Notice that we average the downlink channel parameters over fast fading. Therefore, the beamforming vectors are not updated at the rate of fast fading but at the rate the medium-term downlink channel parameters change. This leads to a significant reduction in computational complexity. Moreover, all processing takes place in the BS.

This paper is organized as follows. The downlink channel parameters can be obtained in different ways as explained in Section 2. Section 3 describes the downlink signal model, and we illustrate the complete downlink data model in Section 4. Section 5 gives the scheme which determines the downlink beamforming vectors. Finally, Section 6 examines the scheme with respect to complexity and bit error ratios by means of Monte-Carlo simulations.

2 Channel Parameter Estimation

In [8], the (medium-term) downlink channel parameter estimates are obtained by feedback information on the uplink. To this end, each antenna element transmits different pilot signals. The channel estimates at each mobile are then transmitted to the BS. To keep feedback rates reasonably low, the estimates are averaged over fast fading.

However, channel information estimated on the uplink can also be applied to the downlink. The frequency offset between up- and downlink in WCDMA is approximately equal to 190 MHz. We assume that the reciprocity between up- and downlink comprises the directions of arrival (DOAs), the delays, and the medium-term average path losses[2]. Note that the reciprocity does not hold for the phases.

Since the DOAs, delays, and medium-term average path losses of the impinging wavefronts are much less time- and frequency-variant than the phases, the medium-term uplink channel information may be obtained by averaging over several consecutive uplink slots [5], i.e., by averaging over fast fading. Moreover, averaging reduces the influence of interference and noise considerably. In [2], we describe how to obtain a signal-and-interference-plus-noise as well as an interference-plus-noise space-frequency covariance matrix for each WCDMA uplink slot and each mobile. In order to obtain the channel parameters listed below, the covariance matrices are averaged and applied to the 3-D channel sounding algorithm based on 3-D Unitary ESPRIT as described in [10].

For downlink processing, the DOAs in terms of azimuth $\phi_{k,\ell}$ and elevation $\theta_{k,\ell}$, the delays $\tau_{k,\ell}$, and the medium-term average path losses $\bar{\alpha}_{k,\ell}$ of the dominant wavefronts ℓ of each mobile k, where $1 \leq \ell \leq L_k$ and $1 \leq k \leq K$, are required. Here, L_k denotes the number of dominant wavefronts of mobile k and K is the number of co-channel mobiles in one cell.

[2]Experimental measurements at 900 MHz have shown that the DOAs remain relatively stable over the frequency range used for uplink and downlink transmission in GSM [1].

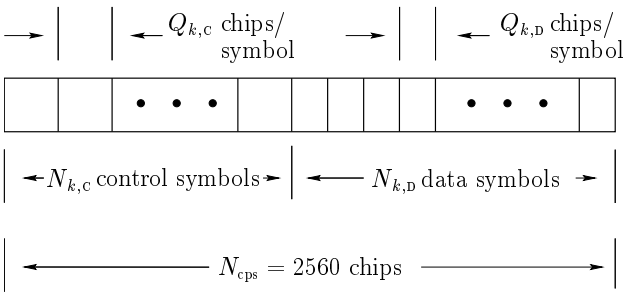

Figure 2: Downlink slot structure of WCDMA for the k-th mobile: The DPDCH and DPCCH are time-multiplexed. The number of chips per slot equals N_{cps}. Moreover, $N_{k,\mathrm{P}}$ dedicated pilot symbols are broadcasted at the beginning of each DPCCH slot. For simplicity, we assume $Q_k = Q_{k,\mathrm{D}} = Q_{k,\mathrm{C}}\ \forall\ k$.

3 Downlink Signal Model

An extensive overview of WCDMA is given in [6, 5]. WCDMA has two types of dedicated physical channels, the dedicated physical control channel (DPCCH) and the dedicated physical data channel (DPDCH). On the downlink, the DPDCH and DPCCH are time-multiplexed, cf. Figure 2. In case of data rates not exceeding 2 Mb/s, one connection consists of one DPCCH and one DPDCH. For the sake of notational simplicity, we assume that the power and spreading codes are identical for the DPDCH and the DPCCH of each mobile. Moreover, we do not include scrambling in our notation. The downlink baseband signal for the mobile k may then be expressed as

$$s_k(t) = \sum_{m=-\infty}^{\infty} b_k^{(m)}\, c_k(t - mT_k), \tag{1}$$

$$c_k(t) = \sum_{q=1}^{Q_k} d_{k,q}\, p(t - qT_c). \tag{2}$$

The chip rate in WCDMA equals $1/T_c = 4.096$ Mchips/s. Moreover, the spreading code, $c_k(t)$, is of length $T_k = Q_k T_c$ and is composed of Q_k chips $d_{k,q} \in \{-1, 1\}$, $1 \leq q \leq Q_k$. The symbols, $b_k^{(m)} \in \{1, \mathrm{j}, -1, -\mathrm{j}\}$, are QPSK modulated. Furthermore, $p(t) \in \mathbb{R}$ denotes the chip-waveform which has a square-root raised cosine spectrum with a rolloff factor of $\alpha = 0.22$.

Notice that downlink transmission is synchronized on the symbol level to exploit the orthogonality of the spreading sequences. Of course, this orthogonality is degraded by multipath propagation. On the other hand, downlink transmission is (intentionally) not synchronized with respect to the slots to be able to take full advantage of discontinous transmission (DTX) or packet services[3].

4 Downlink Data Model

We assume that the mobiles are equipped with a conventional maximum ratio combining rake receiver [11]. The

[3]Note that the DPDCH part of the slot may be empty. However, the control channel is always transmitted due to uplink power control, etc.

required signal to noise and interference ratio after combining in the k-th mobile (SINR_k) is defined according to

$$\mathcal{S}_k = \mathrm{SINR}_k \cdot (\mathcal{I}_k^{\mathrm{au}} + \mathcal{I}_k^{\mathrm{cr}} + \mathcal{N}_k) \ \forall\, k, \tag{3}$$

and must be chosen with respect to the QoS (Quality of Service) requirements. Here, the noise power of the k-th user $\mathcal{N}_k$ comprises the thermal noise and intercell interference. Intracell interference occurs due to intersymbol interference (ISI) and multi-user access interference (MAI). The auto-correlation interference power caused by ISI and the cross-correlation interference power caused by MAI are denoted by $\mathcal{I}_k^{\mathrm{au}}$ and $\mathcal{I}_k^{\mathrm{cr}}$, respectively. If the wavefronts for the mobile k arrive at the mobile with different delays, its rake is able to correct the unknown downlink phases. Then the received and combined signal power at the rake output of mobile k is given by

$$\begin{aligned}\mathcal{S}_k &= \mathrm{E}\left\{ \left(\sum_{n_\mathrm{f}=1}^{N_\mathrm{f}} \left| \sum_{n_\mathrm{z}=1}^{N_\mathrm{z}} \boldsymbol{z}_{k,n_\mathrm{z}}^{\mathrm{H}}\, \boldsymbol{y}_{k,n_\mathrm{f}}^{(k,n_\mathrm{f})} b_k^{(m)} |v_{k,n_\mathrm{f}}| \right| \right)^2 \right\} \\ &= \left(\sum_{n_\mathrm{f}=1}^{N_\mathrm{f}} \left| \sum_{n_\mathrm{z}=1}^{N_\mathrm{z}} \boldsymbol{z}_{k,n_\mathrm{z}}^{\mathrm{H}}\, \boldsymbol{y}_{k,n_\mathrm{f}}^{(k,n_\mathrm{f})} |v_{k,n_\mathrm{f}}| \right| \right)^2,\end{aligned}$$

where[4]

$$\boldsymbol{y}_{k,n_\mathrm{f}}^{(k,n_\mathrm{f})} = \boldsymbol{a}_{k,n_\mathrm{f}} \mathrm{ACF}_k(0).$$

The mobile rake has N_f fingers and the number of downlink beamforming vectors used per mobile equals N_z. The weighted steering vector $\boldsymbol{a}_{k,n_\mathrm{f}} \in \mathbb{C}^M$ depends on azimuth, elevation, and medium-term path loss, cf. Section 2. The subscript k denotes the mobile and M is the number of BS antenna elements. ACF_k and $\mathrm{CCF}_{k,k'}$ stand for the auto-correlation function and the cross-correlation function of the spreading codes c_k and $c_{k'}$, respectively[5]. The downlink beamforming vectors are denoted as $\boldsymbol{z}_{k,n_\mathrm{z}} \in \mathbb{C}^M$. The averaged weight applied to the n_f-th rake finger in the k-th mobile equals $v_{k,n_\mathrm{f}} \in \mathbb{C}$.

If the wavefronts are transmitted at the same time, the N_z beamforming vectors $\boldsymbol{z}_{k,n_\mathrm{z}}$ of the k-th mobile can be merged to one beamforming vector $\boldsymbol{w}_k$ according to

$$\mathcal{S}_k = \left(\sum_{n_\mathrm{f}=1}^{N_\mathrm{f}} \left| \boldsymbol{w}_k^{\mathrm{H}}\, \boldsymbol{y}_{k,n_\mathrm{f}}^{(k,n_\mathrm{f})} |v_{k,n_\mathrm{f}}| \right| \right)^2,$$

where

$$\boldsymbol{w}_k = \sum_{n_\mathrm{z}=1}^{N_\mathrm{z}} \boldsymbol{z}_{k,n_\mathrm{z}}.$$

In general, the wavefronts arrive at each mobile at different times due to different delays τ_{k,n_f}, $1 \le n_\mathrm{f} \le N_\mathrm{f}$, when transmitted at the same time. Here, we assume that the delays differ sufficiently so that the rake receivers are able to resolve the multipaths and, thus, are able to combine coherently.

Of course, the phases of v_{k,n_f} in the mobile rake receiver are not available in the BS since the downlink phases are not known. However, the BS can calculate the averaged absolute value of v_{k,n_f} as follows:

$$|v_{k,n_\mathrm{f}}| = |\, \boldsymbol{w}_k^{\mathrm{H}}\, \boldsymbol{y}_{k,n_\mathrm{f}}^{(k,n_\mathrm{f})} \,| \tag{4}$$

Moreover, the norm of the finger weights of each mobile rake can be chosen freely without influencing its SINR. Therefore, we set

$$\|\boldsymbol{v}_k\|_2 = \left\| [v_{k,1} \quad v_{k,2} \quad \dots \quad v_{k,N_\mathrm{f}}]^{\mathrm{H}} \right\|_2 = 1. \tag{5}$$

The intracell interference in terms of ISI and MAI is caused by non-ideal auto-correlation and cross-correlation properties of the spreading codes c_k according to

$$\begin{aligned}\mathcal{I}_k^{\mathrm{au}} &= \sum_{n_\mathrm{f}=1}^{N_\mathrm{f}} \sum_{\ell=1,\ell\neq n_\mathrm{f}}^{L_k} \left| \boldsymbol{w}_k^{\mathrm{H}}\, \boldsymbol{y}_{k,\ell}^{(k,n_\mathrm{f})} |v_{k,n_\mathrm{f}}| \right|^2, \\ \mathcal{I}_k^{\mathrm{cr}} &= \sum_{k'=1,k'\neq k}^{K} \sum_{n_\mathrm{f}=1}^{N_\mathrm{f}} \sum_{\ell=1}^{L_k} \left| \boldsymbol{w}_{k'}^{\mathrm{H}}\, \boldsymbol{y}_{k,\ell}^{(k',n_\mathrm{f})} |v_{k,n_\mathrm{f}}| \right|^2,\end{aligned}$$

where

$$\begin{aligned}\boldsymbol{y}_{k,\ell}^{(k,n_\mathrm{f})} &= \boldsymbol{a}_{k,\ell} \mathrm{ACF}_k(\tau_{k,n_\mathrm{f}} - \tau_{k,\ell}), \\ \boldsymbol{y}_{k,\ell}^{(k',n_\mathrm{f})} &= \boldsymbol{a}_{k,\ell} \mathrm{CCF}_{k',k}(\tau_{k,n_\mathrm{f}} - \tau_{k',\ell})\end{aligned}$$

hold. Note that the medium-term post-correlation downlink channel vector $\boldsymbol{y}_{k,\ell}^{(k',n_\mathrm{f})}$ is calculated from the averaged channel information estimated on the uplink, cf. Section 2. The number of dominant wavefronts of the k-th mobile is denoted by L_k. In addition to (3), we require the total downlink transmit power

$$P = \sum_{k=1}^{K} \boldsymbol{w}_k^{\mathrm{H}} \boldsymbol{w}_k \tag{6}$$

to be as small as possible in order to reduce the intercell interference.

Fast fading is not taken into account since we use the medium-term downlink channel parameters. However, if the SINR target is not reached (exceeded) at the rake receiver output, power control can trigger an increase (decrease) of the noise and intercell interference power $\mathcal{N}_k$ of mobile k. Macro-diversity which is required for soft handoff can also be taken into account by adapting $\mathcal{N}_k$ of mobile k at the involved base stations[6].

5 Estimation of the Downlink Beamforming Vectors

We must avoid more than one wavefront assigned to a mobile arriving at that mobile at the same time. Otherwise, the rake receiver fails to resolve the impinging wavefronts independently which may lead to combined wavefronts weakened or even eliminated by superposition (noncoherent addition). The simplest approach consists of serving

[4] Here, the wavefronts of each user are transmitted at the same time.

[5] An extension of this notation is required if the spreading factors Q_k are not equal for all K mobiles.

[6] Notice that intercell interference determines the minimum downlink receive power at each mobile, especially if the mobile is close to the cell border.

each mobile only on the strongest multipath component ($N_z = 1$). Without loss of generality, we assume that $\|\boldsymbol{a}_{k,1}\|_2 \geq \|\boldsymbol{a}_{k,\ell}\|_2 \ \forall\ k$ holds for $\ell > 1$. In this case, constraint (5) reduces to $\|v_{k,1}\|_2 = 1 \ \forall\ k$ and can, therefore, be ignored. Equations (3) and (6) take the following form:

Minimize

$$P = \sum_{k=1}^{K} \boldsymbol{w}_k^{\mathrm{H}} \boldsymbol{w}_k \tag{7}$$

subject to

$$\begin{aligned} \|\boldsymbol{w}_k^{\mathrm{H}} \boldsymbol{y}_{k,1}^{(k)}\|_2^2 &= \mathrm{SINR}_k \cdot (\mathcal{I}_k^{\mathrm{cr}} + \mathcal{I}_k^{\mathrm{au}} + \mathcal{N}_k) \\ &= \boldsymbol{w}_k^{\mathrm{H}} \boldsymbol{C}_k \boldsymbol{w}_k \quad \forall \quad k, \end{aligned} \tag{8}$$

where

$$\begin{aligned} \mathcal{I}_k^{\mathrm{au}} &= \sum_{\ell=2}^{L_k} \boldsymbol{w}_k^{\mathrm{H}} \boldsymbol{y}_{k,\ell}^{(k,1)} \boldsymbol{y}_{k,\ell}^{(k,1)\ \mathrm{H}} \boldsymbol{w}_k \\ &= \boldsymbol{w}_k^{\mathrm{H}} \boldsymbol{C}_k^{\mathrm{au}} \boldsymbol{w}_k, \\ \mathcal{I}_k^{\mathrm{cr}} &= \sum_{k'=1, k' \neq k}^{K} \sum_{\ell=1}^{L_k} \boldsymbol{w}_{k'}^{\mathrm{H}} \boldsymbol{y}_{k,\ell}^{(k',1)} \boldsymbol{y}_{k,\ell}^{(k',1)\ \mathrm{H}} \boldsymbol{w}_{k'} \\ &= \sum_{k'=1, k' \neq k}^{K} \boldsymbol{w}_{k'}^{\mathrm{H}} \boldsymbol{C}_{k,k'}^{\mathrm{cr}} \boldsymbol{w}_{k'} \end{aligned}$$

hold. A very similar problem has been examined in [7] for a TDMA system such as GSM enhanced with adaptive antennas at the BS. Several solutions to this problem are listed in [7], e.g., a computationally complex non-linear method such as the augmented Lagrangian algorithm for non-linear equalities. In an SDMA system based on GSM, no more than five mobiles must be taken into account jointly. However, more than 60 mobiles can operate in the same channel in WCDMA. Therefore, it is essential to utilize less complex schemes.

To this end, we rewrite the beamforming vectors as follows:

$$\boldsymbol{w}_k = \sqrt{P_k} \boldsymbol{u}_k \quad \text{and} \quad \|\boldsymbol{u}_k\|_2 = 1 \quad \forall \quad k$$

The basic idea of the following scheme is to transform the joint optimization problem for all K beamforming vectors $\boldsymbol{w}_k$ into K decoupled problems and to separately estimate the normalized beamforming vector $\boldsymbol{u}_k$ and the power P_k required for the k-th mobile. If the constraints given in equation (8) are rewritten according to

$$P_k \boldsymbol{u}_k^{\mathrm{H}} \mathcal{A}_k \boldsymbol{u}_k \ - \sum_{k'=1, k' \neq k}^{K} P_{k'} \boldsymbol{u}_{k'}^{\mathrm{H}} \mathcal{C}_k \boldsymbol{u}_{k'} = 1,$$

where

$$\mathcal{A}_k = \left(\frac{\boldsymbol{C}_k}{\mathrm{SINR}_k \mathcal{N}_k} - \frac{\boldsymbol{C}_k^{\mathrm{au}}}{\mathcal{N}_k} \right) \quad \text{and} \quad \mathcal{C}_{k,k'} = \frac{\boldsymbol{C}_{k,k'}^{\mathrm{cr}}}{\mathcal{N}_k}$$

hold, we can set up the following set of linear equations:

$$\boldsymbol{\Psi} \cdot \begin{bmatrix} P_1 \\ P_2 \\ \vdots \\ P_K \end{bmatrix} = \begin{bmatrix} 1 \\ 1 \\ \vdots \\ 1 \end{bmatrix}, \tag{9}$$

$$\boldsymbol{\Psi} = \begin{bmatrix} \boldsymbol{u}_1^{\mathrm{H}} \mathcal{A}_1 \boldsymbol{u}_1 & -\boldsymbol{u}_2^{\mathrm{H}} \mathcal{C}_{1,2} \boldsymbol{u}_2 & \cdots & -\boldsymbol{u}_K^{\mathrm{H}} \mathcal{C}_{1,K} \boldsymbol{u}_K \\ -\boldsymbol{u}_1^{\mathrm{H}} \mathcal{C}_{2,1} \boldsymbol{u}_1 & \boldsymbol{u}_2^{\mathrm{H}} \mathcal{A}_2 \boldsymbol{u}_2 & \cdots & -\boldsymbol{u}_K^{\mathrm{H}} \mathcal{C}_{2,K} \boldsymbol{u}_K \\ \vdots & \vdots & \ddots & \vdots \\ -\boldsymbol{u}_1^{\mathrm{H}} \mathcal{C}_{K,1} \boldsymbol{u}_1 & -\boldsymbol{u}_2^{\mathrm{H}} \mathcal{C}_{K,2} \boldsymbol{u}_2 & \cdots & \boldsymbol{u}_K^{\mathrm{H}} \mathcal{A}_K \boldsymbol{u}_K \end{bmatrix}$$

Each normalized beamforming vector $\boldsymbol{u}_k$ is the eigenvector corresponding to the positive eigenvalue of the matrix

$$\mathcal{A}_k - \sum_{k'=1, k' \neq k}^{K} \mathcal{C}_{k',k}.$$

Note that each user's transmit signal generates more signal power than interference power if all columns of matrix $\boldsymbol{\Psi}$ add up to be positive. Then the eigenvalue corresponding to the eigenvector which is the normalized beamforming vector $\boldsymbol{u}_k$ must be positive. Moreover, the transmit power P_k for each mobile will also be positive. Since the medium-term channel parameters change slowly, the inversion of $\boldsymbol{\Psi} \in \mathbb{C}^{K \times K}$ which is required to obtain the transmit powers P_k can be performed iteratively [9] at reduced computational complexity.

With initial estimates of the normalized beamforming vectors and the corresponding powers according to (9), we can apply a linear iterative algorithm described in [7] which offers a performance close to the non-linear schemes at a significantly reduced computational complexity.

Notice that the dimension of matrix $\boldsymbol{\Psi}$ is increased by one when a new mobile starts to communicate. However, the system may not be able to meet the service requirements of the new mobile depending on the current load. By evaluating matrix $\boldsymbol{\Psi} \in \mathbb{C}^{(K+1) \times (K+1)}$, we are able to perform admission control very efficiently, since all columns simply must add up to be positive.

6 Simulations

To ensure realistic simulation scenarios, propagation data of the downtown of Munich is utilized generated by a sophisticated ray tracing tool developed at the University of Karlsruhe [4]. The scenario is based on a three-dimensional topographical model of downtown Munich, where the height of the base station is 26 meters and the height of the transmitter at the mobiles is 2 meters, cf. Figure 3.

In the sequel, we assume optimum downlink channel parameter estimation in the BS, i.e., the medium-term post-correlation downlink channel vectors $\boldsymbol{y}_{k,\ell}^{(k',1)}$ have been determined with the ray-trace parameters of $L_k = 5$ dominant wavefronts of each user. Here, we have used long scrambling codes which comprise 40960 chips. Therefore, the signal, auto-, and cross-correlation covariance matrices $\boldsymbol{C}_k$, $\boldsymbol{C}_k^{\mathrm{au}}$, and $\boldsymbol{C}_{k,k'}^{\mathrm{cr}}$ must be averaged over a sufficient number of symbols. Even though the scheme described in Section 5 takes only the dominant multipath component into account for signal transmission, the rakes are equipped with $N_f = 5$ rake fingers which are set to the exact delays

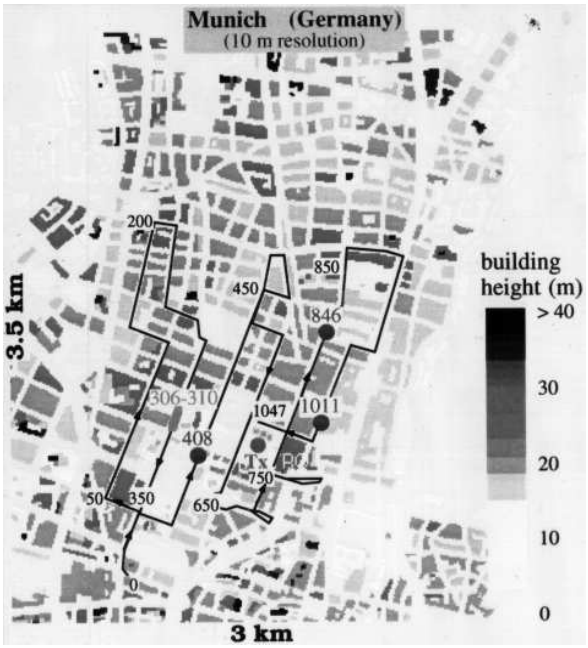

Figure 3: Map of downtown Munich showing the location of the base station (TX) and the mobiles. The propagation data in terms of DOAs, delays, Dopplers, and attenuations of each impinging wavefront is available for 57 different mobile positions.

τ_{k,n_f} and weights v_{k,n_f}. Hence, the SINR at the rake outputs will be slightly better than expected according to (7) and (8). Moreover, it is assumed that the mobiles are not moving. Then the Doppler is zero and (fast) fading does not occur. We chose a scenario with 4 high-data-rate users in one cell with a spreading factor of $Q_k = 16$ which corresponds to a raw data rate of 512 kb/s.

In the first simulation, we only consider intracell interference and set the intercell interference to zero. The raw bit error ratio (BER) of user 1 is plotted as a function of the number of antenna elements (of a uniform linear array) with intracell interference, cf. Figure 5. The target SINR is set to 10 dB for each user. The dashed BER-curve is obtained by calculating the power and normalized beamforming vector for each user separately taking into account only the dominant path. The power is set to the inverse of the attenuation of the dominant path and the normalized beamforming vector is equivalent with the normalized steering vector of the dominant path. We achieve a significant improvement, cf. solid BER-curve in Figure 5, by determining the normalized beamforming vector and the corresponding transmit power by jointly considering all mobiles in the cell according to equation (9), thus serving each mobile on its strongest multipath component. In both cases, users 2, 3, and 4 had a BER of zero. In Figure 4, the beamforming patterns of user 1 and user 2 are plotted with dashed and solid lines in case of separately taking into account the dominant path of each user and in case of utilizing equation (9), respectively. By taking into account the correlation properties, the beamforming patterns of users 2, 3, and 4 change significantly which corresponds with the improvements seen in Figure 5 for user 1. Obviously, user 1 is the weakest of the 4 users since its beamforming pattern does not change.

In the next simulation, we take strong intercell interference into account as well, cf. Figure 5. Intercell interference (and thermal noise) is modeled as white additive Gaussian noise and the signal to noise ratio (SNR) at the receiving antenna of the mobile (before the correlator) is set to 0 dB. Accordingly, the improvements attained by calculating the beamforming vectors and corresponding transmit powers with equation (9) are less pronounced.

7 Conclusion

In general, separation is neither orthogonal in space nor by code in contrast to separation in frequency or time. Here, the mobiles are separated not only by code or space but by code *and* space. Therefore, we have presented a data model for WCDMA that takes into account BS adaptive antennas and comprises the correlation properties of the codes as well as the spatial and temporal downlink channel parameters. Preliminary simulation results have shown that the performance and, thus, the capacity can be increased significantly by taking into account the correlation properties.

References

[1] L. Bigler, H. P. Lin, S. S. Jeng, and G. Xu, "Experimental direction of arrival and spatial signature measurements at 900 MHz for smart antenna systems", in *Proc. IEEE Vehicular Techn. Conf.*, pp. 55–58, Chicago, IL, July 1995.

[2] C. Brunner, M. Haardt, and J. A. Nossek, "2-D rake receiver in the space-frequency domain for the uplink of WCDMA", in *Proc. 6th IEEE International Workshop on Intelligent Signal Processing and Communication Systems. (ISPACS '98)*, vol. 2, pp. 551–555, Melbourne, Australia, Nov. 1998.

[3] C. Brunner, M. Haardt, and J. A. Nossek, "Adaptive space-frequency rake receivers for WCDMA", in *Proc. IEEE Int. Conf. Acoust., Speech, Signal Processing*, Phoenix, Arizona, Mar. 1999, accepted for publication.

[4] D. J. Cichon, *Strahlenoptische Modellierung der Wellenausbreitung in urbanen Mikro- und Pikofunkzellen*, Ph. D. dissertation, University of Karlsruhe, Karlsruhe, Germany, Dec. 1994, in German.

[5] E. Dahlman, B. Gudmundson, M. Nilsson, and J. Sköld, "UMTS/IMT-2000 based on wideband CDMA", *IEEE Communication Magazine*, vol. 36, pp. 70–80, Sept. 1998.

[6] E. H. Dinan and B. Jabbari, "Spreading codes for direct sequence CDMA and wideband CDMA cellular networks", *IEEE Communication Magazine*, vol. 36, pp. 48–54, Sept. 1998.

[7] C. Farsakh and J. A. Nossek, "Spatial covariance based downlink beamforming in an SDMA mobile radio system", *IEEE Trans. Communications*, vol. 46, pp. 1497–1506, 1998.

[8] D. Gerlach and A. Paulraj, "Base station transmitting antenna arrays for multipath environments", *Signal Processing*, vol. 54, pp. 59–74, Oct. 1996.

[9] G. H. Golub and C. F. van Loan, *Matrix Computations*, Johns Hopkins University Press, Baltimore, MD, 2nd edition, 1989.

[10] M. Haardt, C. Brunner, and J. A. Nossek, "Efficient high-resolution 3-D channel sounding", in *Proc. 48th IEEE Vehicular Technology Conf. (VTC '98)*, pp. 164–168, Ottawa, Canada, May 1998.

[11] J. G. Proakis, *Digital Communications*, McGraw-Hill, New York, NY, 2nd edition, 1989.

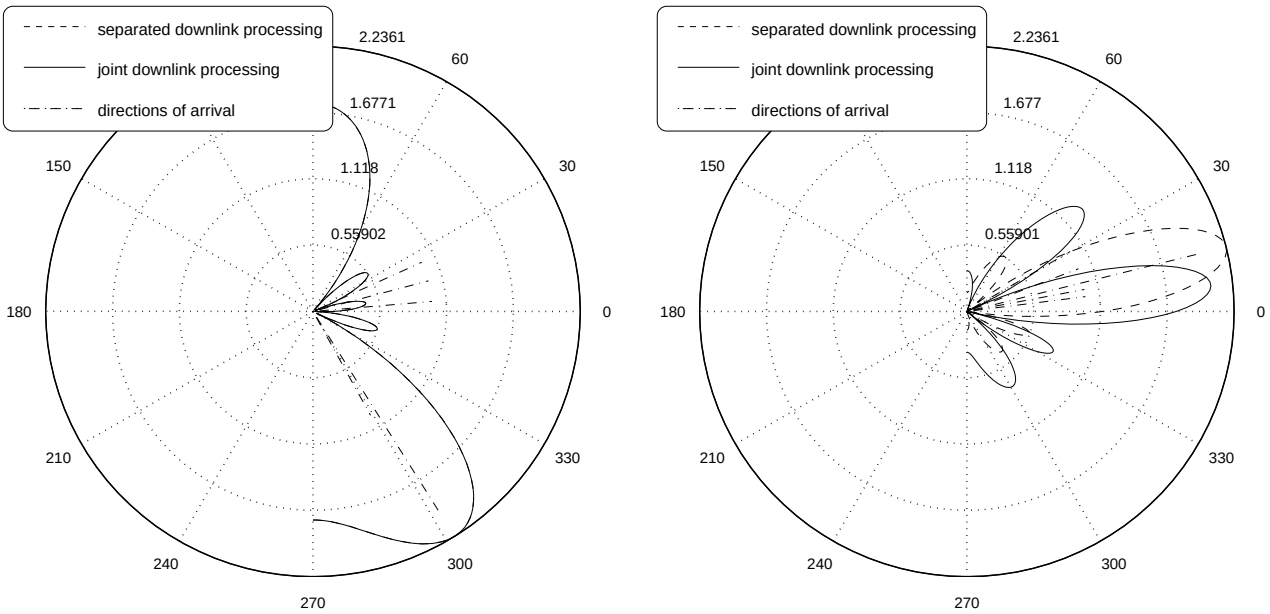

Figure 4: The beamforming patterns of user 1 and user 2 are plotted on the left and right side, respectively. The dashed (normalized) pattern is obtained by taking the dominant path into account for each user separately (separated downlink processing), whereas the solid (normalized) pattern is determined by solving equation (9) (joint downlink processing). The directions of arrival are plotted as dashed lines. Note that the length does not indicate the attenuation but only which path is dominant. By taking into account the correlation properties, the beamforming pattern of user 2 changes significantly. On the other hand, the beamforming pattern of user 1 does not change. (The dashed and solid curves on the left side are the same.) These plots are based on a uniform linear array with $M = 5$ antenna elements.

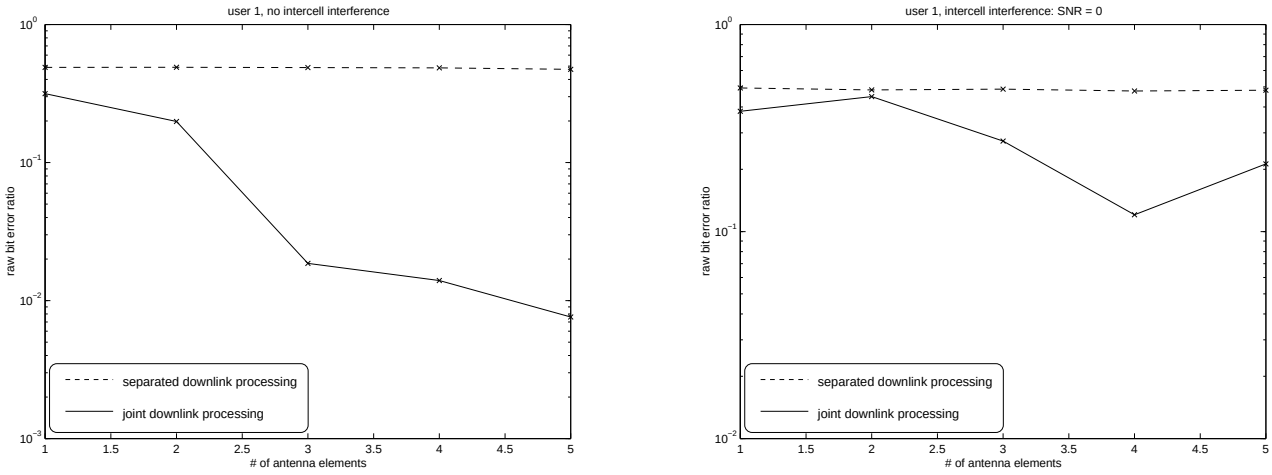

Figure 5: The raw bit error ratio of user 1 is plotted as a function of the number of antenna elements (of a uniform linear array) with intracell interference (on the left), and (on the right) with intracell and intercell interference. Intercell interference (and thermal noise) is modeled as white additive Gaussian noise. The dashed curves are obtained when taking the dominant path of each user into account separately, whereas the solid curves are based on the beamforming vectors and corresponding transmit powers determined by equation (9).